

# An Approach to the Optimization of the Ackerberg-Mossberg's Biquad Circuitry

Martin Pospisilik, Pavel Varacha

**Abstract**— This paper describes a perspective approach to the electrical circuits design based on the utilization of the evolutionary algorithms. In order to show an example of how the devices of a circuit being described by a mathematical model can be determined, a low pass filter design was chosen, employing the circuitry consisting of two integrators in a feedback loop operating as a filter realizing a general biquadratic function. The modified Ackerberg-Mossberg's topology was used. In the paper not only the results of the optimisation but also the results of simulation of the designed circuits are provided, including the sensitivity analysis.

**Keywords**—Evolutionary algorithm, SOMA, Optimization, Biquads, Electrical filters.

## I. INTRODUCTION

THE theory presented in this paper can be divided into two separate subchapters, one dealing with the theory of biquads, especially of the Ackerberg-Mossberg's topology, and the second one dealing with the theory of the artificial intelligence algorithms.

### A. Biquads

Generally, the more complex electrical filters are built of blocks that are realized by means of the second-order elementary filters. These elementary filters usually realize one of the “standard transfer functions” that are described below. The transfer function of the second-order low pass filter can be expressed as:

$$H_{LP}(p) = \frac{k\omega_0^2}{p^2 + \frac{\omega_0}{Q}p + \omega_0^2} \quad (1)$$

The transfer function of the second-order high pass filter can be expressed as:

$$H_{HP}(p) = \frac{kp^2}{p^2 + \frac{\omega_0}{Q}p + \omega_0^2} \quad (2)$$

Martin Pospisilik is with Faculty of Applied Informatics, Tomas Bata University in Zlin, Namesti Tomase Garrigua Masaryka, 76001 Zlin, Czech Republic. (phone: +420 57-603-5228; e-mail: [pospisilik@fai.utb.cz](mailto:pospisilik@fai.utb.cz)).

Pavel Varacha is with Faculty of Applied Informatics, Tomas Bata University in Zlin, Namesti Tomase Garrigua Masaryka, 76001 Zlin, Czech Republic. (e-mail: [varacha@fai.utb.cz](mailto:varacha@fai.utb.cz)).

This paper is supported by the Internal Grant Agency at TBU in Zlin, project No. IGA/FAI/2012/056 and by the European Regional Development Fund under the project CEBIA-Tech No. CZ.1.05/2.1.00/03.0089.

The transfer function of the second-order band-pass filter is expressed as:

$$H_{BP}(p) = \frac{k\frac{\omega_0}{Q}p}{p^2 + \frac{\omega_0}{Q}p + \omega_0^2} \quad (3)$$

The variables in the above enlisted functions are of the following meaning:

- $p$  - complex frequency ( $p = j\omega$ ),
- $\omega_0$  - cutoff frequency [rad/s],
- $k$  - constant (amplification),
- $Q$  - Q factor.

In fact, the functions (1), (2) and (3) are the special case of one “biquadratic” function that is expressed below:

$$H(p) = \frac{a_2p^2 + a_1p + a_0}{p^2 + d_1p + d_2} = \frac{a_2p^2 + a_1p + a_0}{p^2 + \frac{\omega_0}{Q}p + \omega_0^2} \quad (4)$$

where  $a_0, a_1, a_2, d_1, d_2$  are general coefficients. The functional blocks that realize the any case of the biquadratic function are called biquads [1].

During the development of the filters theory and implementation, various ways of how to create an optimal filter were explored, including the filters based on the biquadratical functional blocks. The main requirements were as follows:

- manufacturability of the circuitry,
- good reproducibility of the circuitry and the related low sensitivity of the circuit to the device parameters change,
- possibility of tuning the  $\omega_0$  and  $Q$  parameters separately in order the calibration of the circuits could be processed simply when manufactured.

During the time, several types of the selective functional block based on the biquads have been developed. Generally, they can be divided according to the number of the operational amplifiers employed in order one biquad was created.

The simplest functional blocks employ only one operational amplifier, resulting into low-cost manufacturability, but limited performance. The  $Q$  factor of these circuits must be kept at low values in order the sensitivity of the circuit to the device parameters drift was acceptable. Moreover, the amplification factor of such filters cannot be of the arbitrary

value but its level is usually determined by the other required parameters of the filter.

The more sophisticated functional block were therefore developed in order the above mentioned disadvantages were canceled. The biquads based on two operational amplifiers are usually based on the passive LC filter behavior simulation. Antonio's general impedance converter is usually employed in order the inductor could be replaced by a capacitor [1].

Because of the increased availability of the sufficient operational amplifiers and their possibility of integration on a chip the biquads with more than two operational amplifiers were also developed. From the various range of topologies the biquads employing two integrators in the feedback loop are the most utilized ones [1], including the Tow-Thomas' biquad and Ackerberg-Mossberg's biquad. Such universal biquads can be described by means of the signal diagram depicted in Fig. 1.

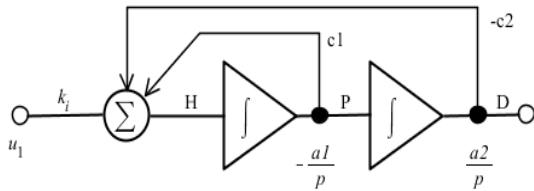


Fig. 1 – Diagram of the signal paths in biquads employing two integrators in the feedback loop [1]

The structure depicted in Fig. 1 provides the relevant outputs at the points marked as H (high-pass output), P (band-pass output) and D (low-pass output). According to [1], the relevant transfer functions are as follows:

$$H_{LP}(p) = \frac{U_D}{U_1} = \frac{k_i a_1 a_2}{p^2 + a_1 c_1 p + a_1 a_2 c_2} = \frac{h \omega_0^2}{p^2 + p \frac{\omega_0}{Q} + \omega_0^2} \quad (5)$$

$$H_{PP}(p) = \frac{U_P}{U_1} = \frac{-k_i a_1 p}{p^2 + a_1 c_1 p + a_1 a_2 c_2} = \frac{-h p \frac{\omega_0}{Q}}{p^2 + p \frac{\omega_0}{Q} + \omega_0^2} \quad (6)$$

$$H_{HP}(p) = \frac{U_H}{U_1} = \frac{k_i p^2}{p^2 + a_1 c_1 p + a_1 a_2 c_2} = \frac{-h p \frac{\omega_0}{Q}}{p^2 + p \frac{\omega_0}{Q} + \omega_0^2} \quad (7)$$

The main advantage of the biquad structure depicted in Fig. 1 is obvious – with the same internal circuitry the filter can be utilized as low-pass, high-pass or band-pass without any change. Due to this phenomenon such structure is often employed in integrated or hybrid circuits.

#### 1) Ackerberg-Mossberg's biquads

The Ackerberg-Mossberg's biquads employ the structure depicted in Fig. 1 but with a modification according to Fig. 2,

where the input summer is brought together with the first integrator.

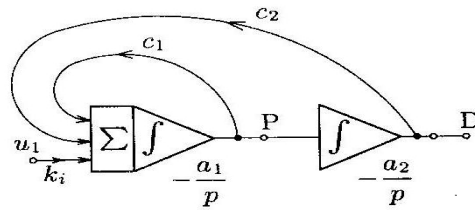


Fig. 2 – Modified arrangement of the biquad employing two integrators in the feedback loop, typical for Ackerberg-Mossberg's biquad construction [1]

The time constants of the integrators depicted in Fig. 3 can be described as follows:

$$\tau_i = \frac{1}{a_i}, \quad i = 1, 2 \quad (8)$$

By further modifications according to [1] the modified connection of the Ackerberg-Mossberg's biquad can be obtained, utilizing the arrangement with one output and more inputs. It is depicted in Fig. 3. This circuit realizes a biquadratic transfer function, having the input in the point marked as  $u_i$  and the output at the point marked as X. Its transfer function can then be expressed as follows:

$$H(p) = \frac{U_x}{U_i} = \frac{p^2 \frac{C2}{C1} + p \omega_0 \left( \frac{R7}{R4} - \frac{R8}{R7} \right) + \frac{R6}{R7} \omega_0^2}{p^2 + p \omega_0 \frac{R7}{R1} + \omega_0^2} \quad (9)$$

In order the (9) was valid; the following condition must be obtained:

$$R_7 = R_5 \quad (10)$$

$$C_2 = C_3 \quad (11)$$

Provided the condition (9) is fulfilled, the following equations can also be applied:

$$\omega_0 = \frac{1}{R_5 C_2} \quad (12)$$

$$Q = \frac{R_1}{R_5} \quad (13)$$

$$k_i = \frac{R_5}{R_4} \quad (14)$$

Although the selection of R2 and R3 is not discussed in [1], they cannot be arbitrary. By simulation it has been proven that these resistors create a load that spoils the performance of the circuit. It became sufficient to set the value of these resistors according to the value of R7.

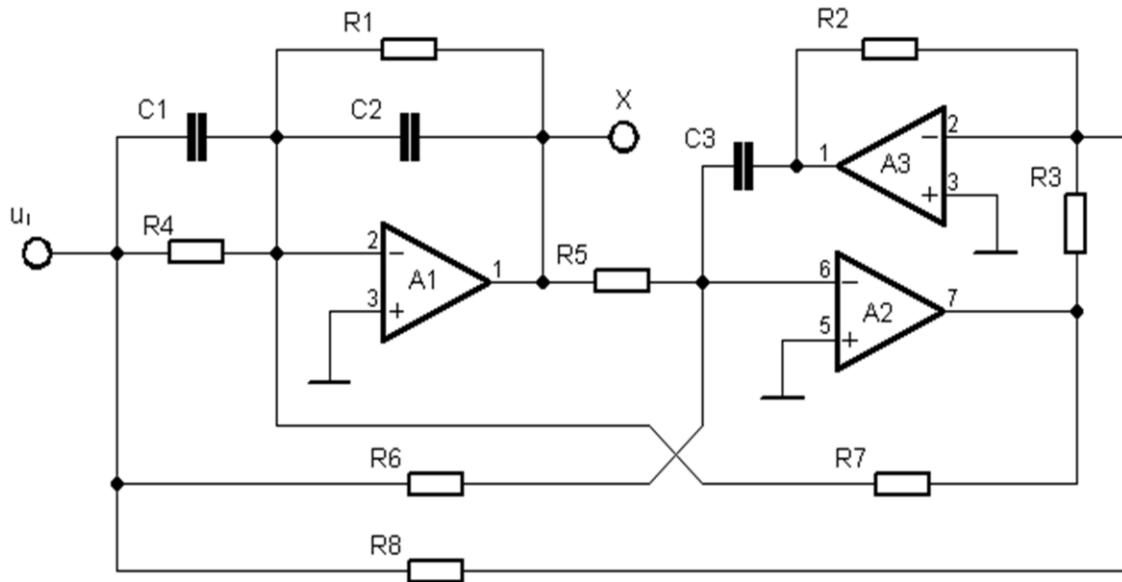


Fig. 3 - Modified connection of the Ackerberg-Mossberg's biquad according to [1]

In practice the following values of  $R_2$  and  $R_3$  can be considered as sufficient:

$$R_2 \cong R_7; R_3 = R_2 \quad (14)$$

In this paper the possibility of setting all the device values of the circuit depicted in Fig. 3 by means of the evolutionary algorithms are described.

### B. Evolutionary algorithms

Evolutionary algorithms are stochastic methods of optimization inspired by the principles of natural evolution. Therefore these algorithms utilize mechanisms of biological evolution – reproduction, mutation, recombination and selection. Currently, many types of evolutionary algorithms are being explored and utilized. In the optimisation described in this paper, the Self-Organizing Migrating Algorithm was employed.

#### 1) Self-Organizing Evolutionary Algorithm

SOMA is based on a self-organizing behaviour of groups of individuals in a “social environment”. It can also be classified as an evolutionary algorithm [4], despite the fact that no new generations of individuals are created during the search (due to the philosophy of this algorithm). Only the positions of individuals in the searched space are changed during one generation called a “migration loop”. The algorithm was published in journals and books, presented at international conferences and symposiums and mentioned in numerous introductory presentations, for example [5], [6], [7].

Although several different versions of SOMA exist, this thesis is focused on the most common All-to-One version, which is suitable for the asynchronous parallel implementation. This chapter describes all basic All-to-One SOMA principles.

## II. THE OPTIMIZATION TASK

In order to check the possibility of optimization of the Ackerberg-Mossberg's biquad connected according to Fig. 3, the optimization task described in this chapter has been processed.

The optimization task consists in searching for the optimal transfer function of a low pass filter based on the Ackerberg-Mossberg's biquad. The Self-Organising Migrating Algorithm was employed to find the most suitable combination of device values in the circuit that is depicted in Fig. 2 according to the desired parameters of the filter.

### A. The required filter parameters

In order to design the low-pass filter as described above the following parameters must be specified:

- $f_p$  – passband limit [Hz] for a 3 dB attenuation,
- $f_n$  – stopband limit for the specified attenuation  $A_{min}$ ,
- $A_{max}$  - maximum overshoot of the response,
- $A_{min}$  – desired attenuation in the stopband.

Based on these parameters, the appropriate values of circuit devices from Fig. 2 are searched for.

In the presented task the parameters were defined as follows:

- $f_p = 1,500$  Hz

- $f_n = 3,000 \text{ Hz}$
- $A_{max} = + 3 \text{ dB}$
- $A_{min} = - 20 \text{ dB}$ .

The graphical expression of the parameters can be found in Fig. 4.

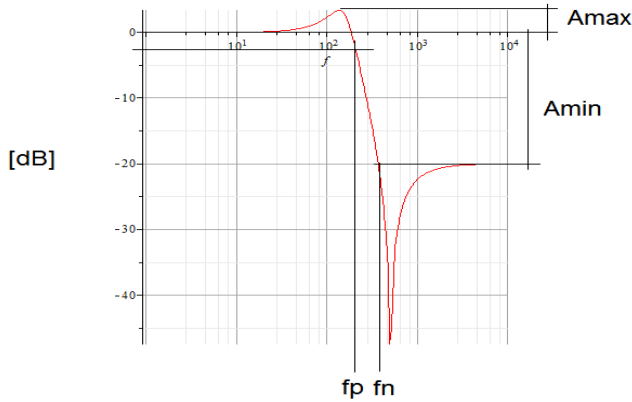


Fig. 4 – Description of the required filter parameters

**B. SOMA Algorithm and its setting**

Before starting the algorithm, the following SOMA parameters must be defined:

- Step,
- PathLength,
- PopSize,
- PRT
- Cost Function.

The Cost Function is simply the function which returns a scalar that can directly serve as a measure of fitness. In this case, Cost Function is provided by AP.

The population of individuals is randomly generated. Each parameter for each individual has to be chosen randomly from a Specimen which defines a range <Low, High> and a value type (integer, double) for each individual’s dimension.

Each individual from a population (PopSize) is evaluated by the Cost Function and the Leader (individual with the highest fitness) is chosen for the current migration loop. Then, all other individuals begin to jump, (according to the Step definition) towards the Leader. Each individual is evaluated after each jump by using the Cost Function. Jumping continues until a new position defined by the PathLength is reached. The new position  $x_{i,j}$  after each jump is calculated by **Chyba! Nenalezen zdroj odkazů.** as is shown graphically in **Chyba! Nenalezen zdroj odkazů.** Later on, the individual returns to the position on its path, where it found the best fitness.

$$x_{i,j}^{MLnew} = x_{i,j,start}^{ML} + (x_{L,j}^{ML} - x_{i,j,start}^{ML})tPRTVector_j \quad (15)$$

Where:  $t \in <0, \text{by Step to, PathLegth}>$  and ML is actual migration loop.

Before an individual begins jumping towards the Leader, a random number  $rnd$  is generated (for each individual’s component), and then compared with PRT. If the generated random number is larger than PRT, then the associated component of the individual is set to 0 using PRTVector. This can be described by the following equation:

$$PRTVector_j = \begin{cases} 0 \Leftrightarrow rnd_j < PRT \\ 1 \Leftrightarrow rnd_j \geq PRT \end{cases} \quad (16)$$

$$rnd \in <0,1>, j = 1, \dots, n_{param}$$

An example of a PRTVector for 4 parameters individual with  $PRT = 0.3$  is enlisted in the table below:

Tab. 1 – Example of a PRTVector

J	$rnd_j$	PRTVector
1	0,234	1
2	0,545	0
3	0,865	0
4	0,012	1

In the figure below, PRTVector and its action on individual movement is depicted.

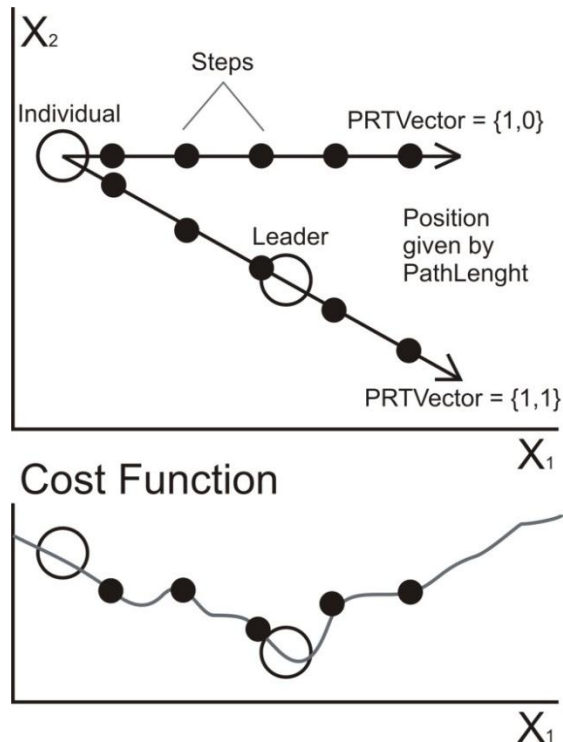


Fig. 5 - PRTVector and its action on individual movement

Hence, the individual moves in the N-k dimensional subspace which is perpendicular to the original space. This fact establishes a higher robustness of the algorithm. Earlier experiments demonstrated that without the use of PRT, SOMA

tends to determine a local optimum rather than a global one. [Chyba! Nenalezen zdroj odkazů..  
 If a stopping condition (time limit, sufficient fitness achieved, number of ML, etc.) is archived, stop and recall the best solution(s) found during the search.

The SOMA explanation chart is depicted in the following figure.

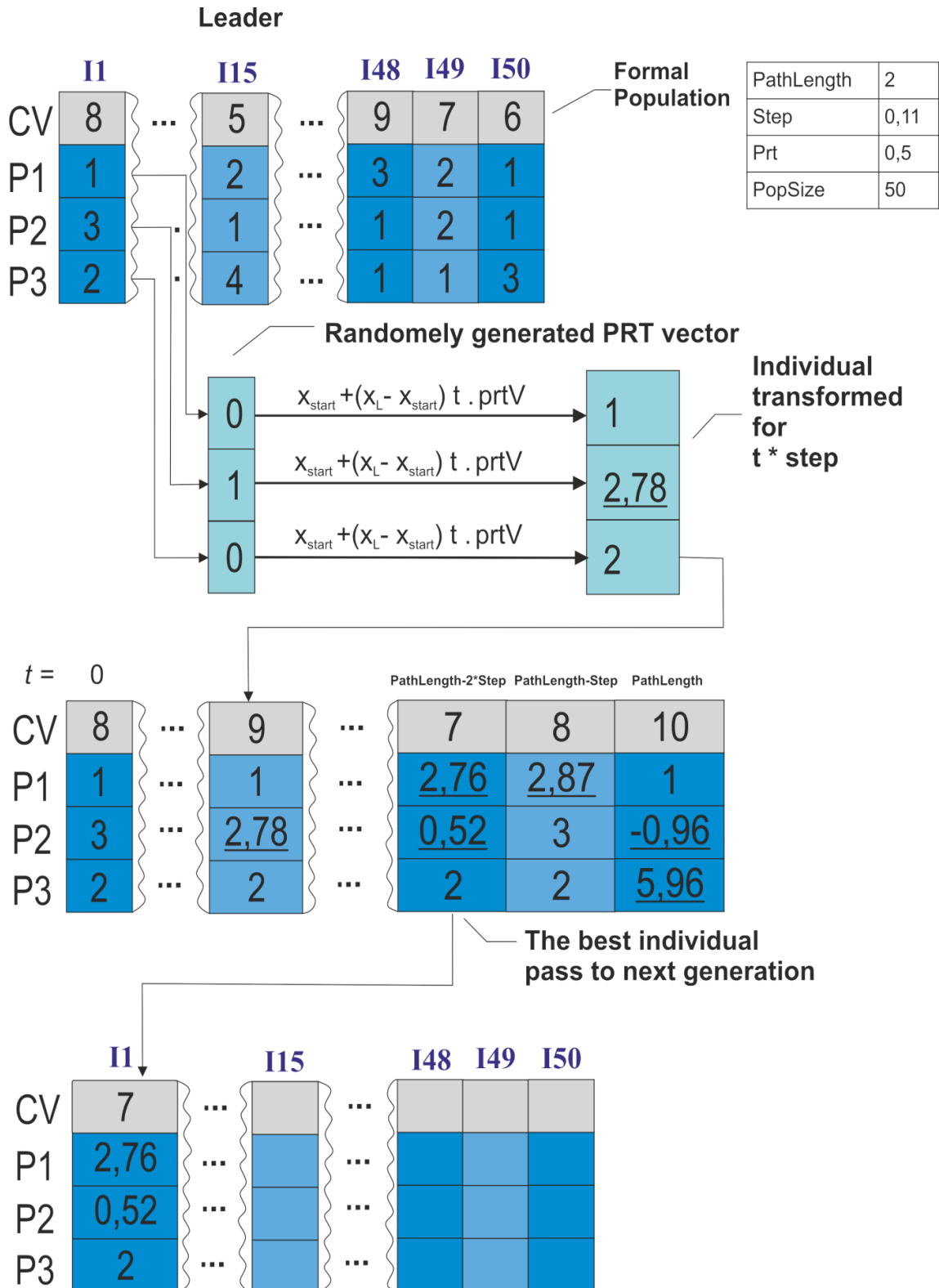


Fig. 6 – SOMA explanation chart

In [8] the author of the Self-Organizing Migrating Algorithm recommends its settings according to the Table 2.

Tab. 2 - SOMA parameters and their recommended domain

Parameter name	Recommended range
PathLenght	<1.1 ;3>
Step	<0.11, PathLength>
PRT	<0,1>
PopSize	<10, up to user>

For the purposes of the optimisation presented in this paper, the parameters of the algorithm setting were modified according to Table 3.

Tab. 3 - SOMA parameters and their settings

Parameter name	Recommended range
PathLenght	3
Step	0.11
PRT	0.125
PopSize	60

The limits of the processed variables were set according to Table 4.

Tab. 4 - Variable's limits

Variable name	Min	Max
C1	$10 \cdot 10^{-12}$	$10 \cdot 10^{-6}$
C2	$10 \cdot 10^{-12}$	$10 \cdot 10^{-6}$
R1	100	$10^6$
R4	100	$10^6$
R6	100	$10^6$
R7	100	$10^6$
R8	100	$10^6$
omega	<b>0.01 * 1500</b>	<b>10 * 3000</b>

According to the parameters presented in the tables above, the final cost function was created as a code in C++ language. Due to its complexity, the printout of the cost functions exceeds the range of this paper.

### C. Verification

All the equations presented in this paper were implemented in Maple computing software and the results gained by the Self-Organizing Migrating Algorithm were substituted into them.

Consequently the graphs of the frequency response of the circuit were obtained.

Moreover an accurate software simulation of the designed filter was processed.

### III. RESULTS DISCUSSION

The results given by the SOMA algorithm are shown in the table below. The proposed values were corrected to the nearest available values from the E12 series [14] and the resulting frequency response was plotted as well. The E12 series was selected for the ease of obtaining of such devices. Moreover the authors would have liked to present how the difference between the accurate values that were proposed by the SOMA algorithm and the values that are physically available affects the resulting response. Both frequency responses are to be seen in Fig. 4. These frequency responses were obtained directly by computing the transfer function for the proposed device values in the Maple software.

Tab. 5 – Results provided by the Self Organizing Migrating Algorithm

Device number	Device values	
	<i>SOMA proposed value</i>	<i>E12 value</i>
R1	523 318 $\Omega$	560 k $\Omega$
R2	Optional	47 k $\Omega$
R3	R2	47 k $\Omega$
R4	489 101 $\Omega$	470 k $\Omega$
R5	416 332 $\Omega$	390 k $\Omega$
R6	305 355 $\Omega$	330 k $\Omega$
R7	416 332 $\Omega$	390 k $\Omega$
R8	323 340 $\Omega$	330 k $\Omega$
C1	7.6563 $\mu\text{F}$	8.2 $\mu\text{F}$
C2 = C3	491.086 nF	0.47 $\mu\text{F}$

Unfortunately, during accurate simulations it became obvious that there are more possible solutions proposed by the SOMA algorithm but only one of them is physically realizable. This phenomenon showed that not only the value of R5 must be specified according to equations (5), (6) and (7), but the iterative verification must be processed as well. Therefore the results presented in the paper indicate that it is possible to apply the Self-Organizing Migrating Algorithm at the design of Ackerberg-Mossberg's biquads right on the basis of the requested transfer function description, but more complex algorithm must be created in order all the values proposed by the algorithm were utilizable without additive verification.

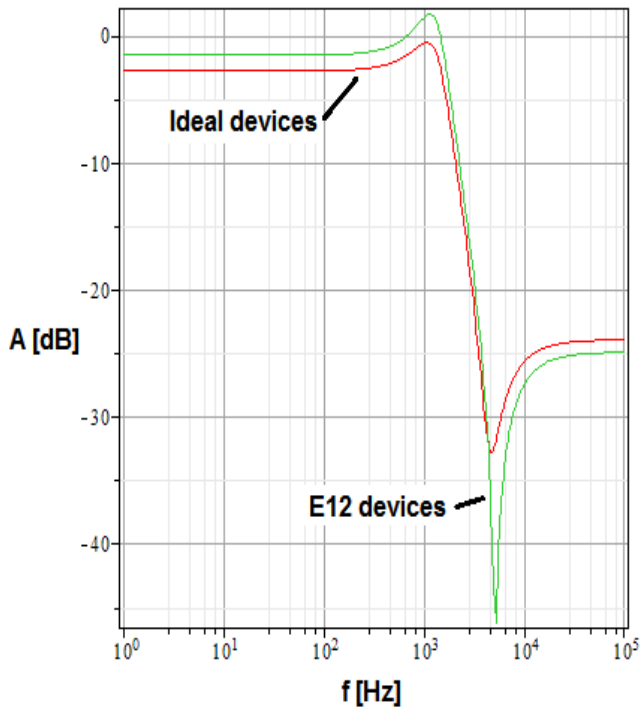


Fig. 7 - Frequency response of the filter designed by SOMA (a – ideal devices) and modified to really available devices from E12 series (b – E12 devices)

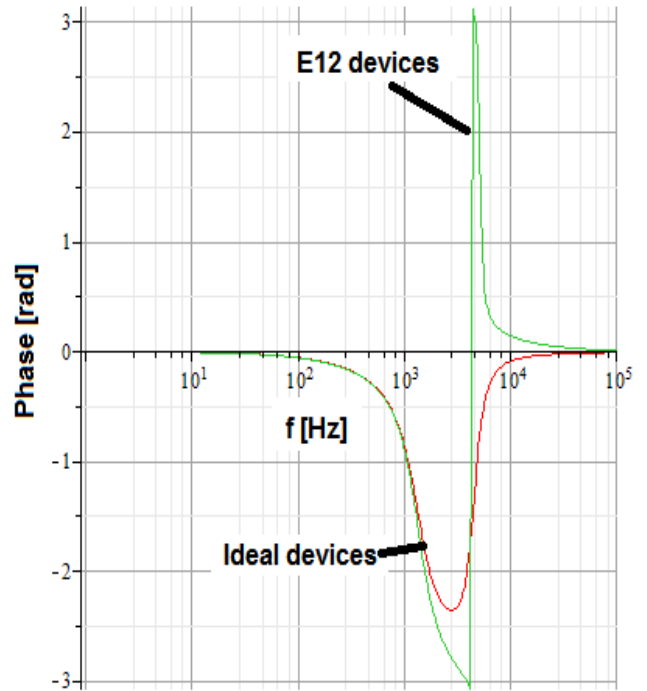


Fig. 8 – Phase response of the filter designed by SOMA (a – ideal devices) and modified to really available devices from E12 series (b – E12 devices)

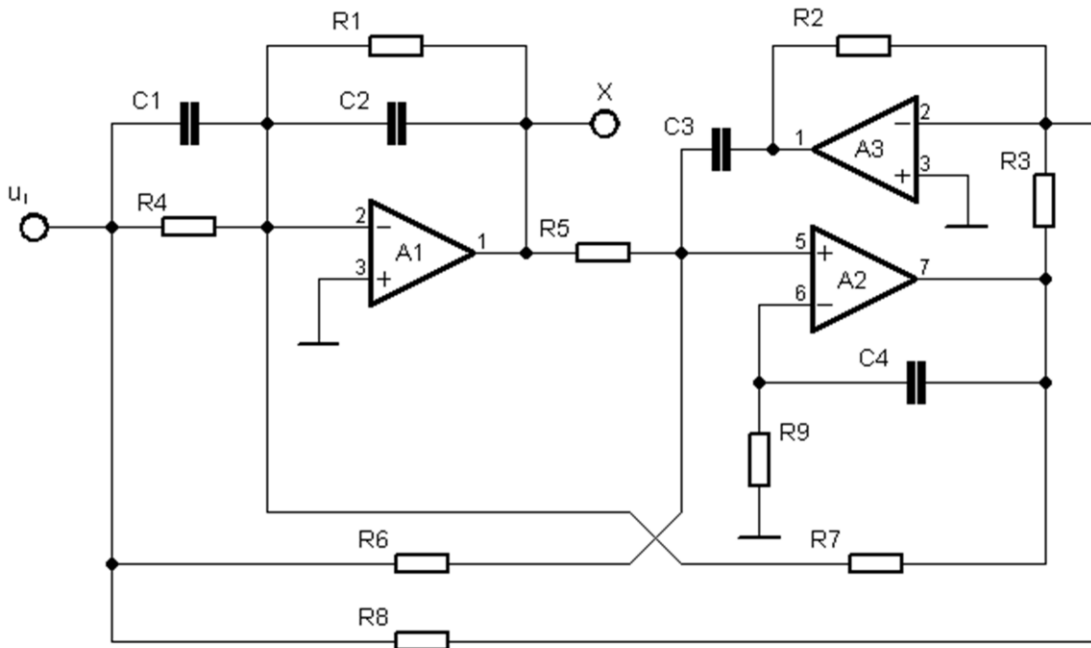


Fig. 9 - Modified connection of the Ackerberg-Mossberg's biquad finally used in the simulation

When comparing the results obtained for the filter constructed with ideal devices and real devices the values of which comply to the E12 series it is clearly apparent that although the frequency responses are quite similar and both comply to the requirements, the phase response of the filter constructed with E12 series devices indicates a large phase shift in the vicinity of the  $\omega_0$  frequency. This may probably result in the lack of the circuit stability. Accurate simulation or more complex computations are needed to check the circuit stability issues.

#### A. Simulation

Generally it can be said that the simulation confirmed the assumptions, but a minor modification of the circuit has had to be introduced in order to increase its stability. The filter circuitry was simulated using the real model of the operational

amplifier TL084. The circuitry tended to be unstable at the frequencies close to the transition frequency of the utilized operational amplifier. Therefore the gain of the operational amplifier A2 has been decreased at high frequencies by implementing the resistor  $R9 = 10 \text{ k}\Omega$  and the capacitor  $C4 = 10 \text{ pF}$ . The final connection of the simulated circuitry is depicted in Fig. 6.

The instability of the circuit when the E12 devices were applied was not confirmed. On the other hand the critical influence of the value of the resistors  $R2$  and  $R3$  to the performance of the circuit has been observed. In Fig. 7 the simulation results for the E12 devices as enlisted in Table 1 is depicted. In the further figures, the sensitivity to the device parameters changes is shown as well as the response of the circuit to the unit step, indicating the stability of the circuit.

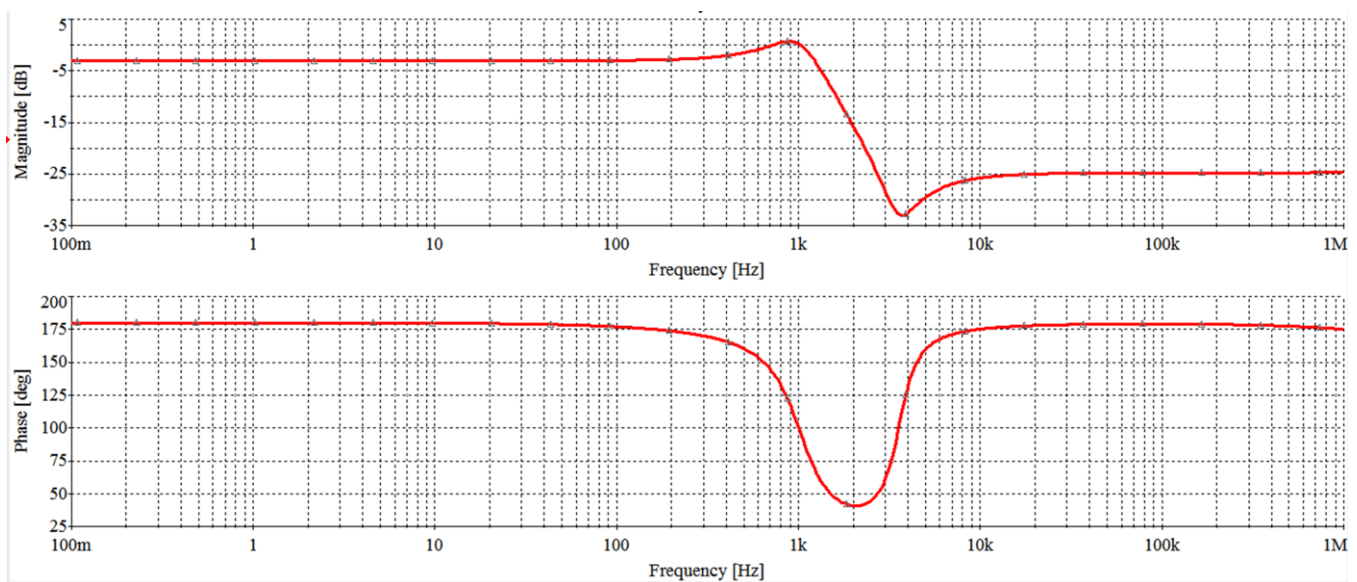


Fig. 7 - Bode plots resulting from the AC simulation of the circuit depicted in Fig. 6 employing the devices described in Table 5

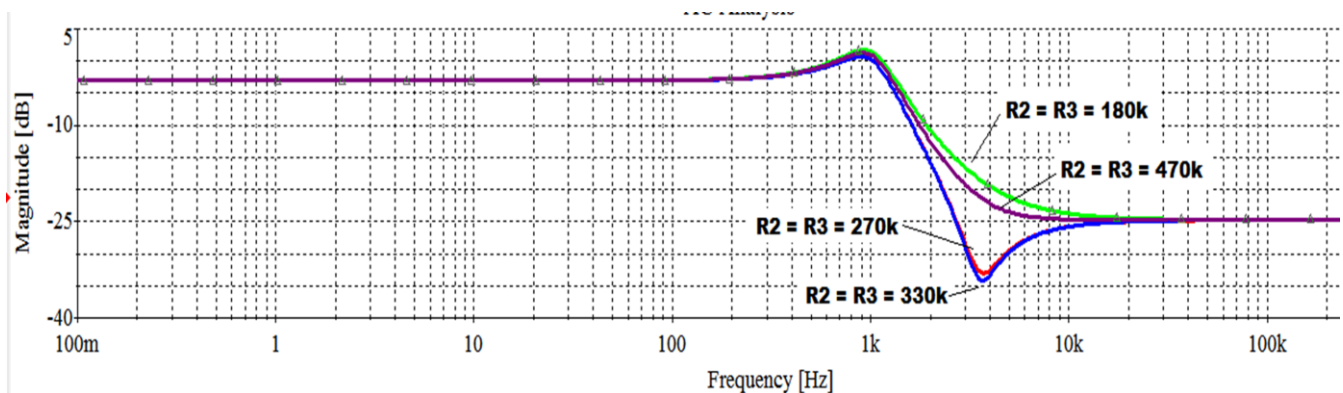


Fig. 8. Influence of the  $R2$  and  $R3$  selection to the filter performance



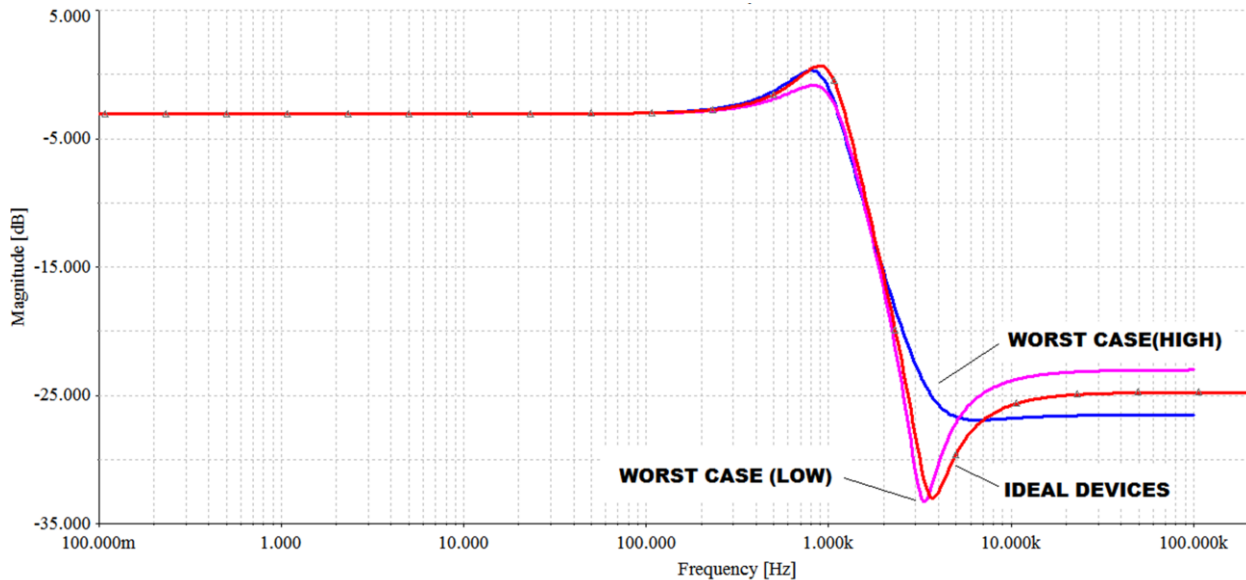


Fig. 9. Worst case analysis (device tolerances  $\pm 10\%$ )

#### IV. CONCLUSION

In this paper the approach to the artificial intelligence-based optimisation of a biquadratic filter constructed according to the Ackergberg-Mossberg's connection is described. The values of the devices used in the filter circuit were found directly by means of the Self-Organizing Migrating Algorithm, according to its transfer function description (9) that was deduced according to the theory presented in [1].

The obtained results were acquired to simulations using SPICE models of the devices, including the model of a real operational amplifier. The results of the simulations are also included in this paper. According to the simulations it can be stated that the results obtained by the evolutionary algorithm were utilizable and the designed filter could be manufactured after minor amendments.

#### REFERENCES

- [1] MARTINEK,P., BORES, P., HOSPODKA, J., Electrical filters [Elektrické filtry], Czech Technical University in Prague, 1. Edition, pp. 89 – 142, 2003, ISBN 80-01-02765-1
- [2] POSPISILIK,M., KOURIL, L., ADAMEK,M., “Planar Inductor Optimised by Evolutionary Algorithm”. In Proceedings of the 17th International Conference on Soft Computing Mendel 2011, 1. Edition., Brno: Faculty of Mechanical Engineering, Institute of Automation and Computer Science, 2011, pp. 38 – 42. ISBN 978-80-214-4302-0
- [3] ZELINKA,I., “SOMA - Self-Organizing Migrating Algorithm“. In New Optimization Techniques in Engineering. Springer, 2004. ISBN: 978-3-540-20167-0.
- [4] KRÁL E., ET AL., Usage of PSO Algorithm for Parameters Identification of District Heating Network Simulation Model. In 14th WSEAS International Conference on Systems. Latest Trends on Systems. Volume II, Rhodes, WSEAS Press (GR) , 2010. p. 657-659. ISBN/ISSN: 978-960-474-214-1.
- [5] ČERVENKA M., ZELINKA I., Application of Evolutionary Algorithm on Aerodynamic Wing Optimisation. In Proceedings of the 2nd European Computing Conference, Venice, WSEAS Press (IT), 2008, ISBN/ISSN: 978-960-474-002-4
- [6] OPLATKOVÁ Z., ZELINKA I., Investigation on Shannon - Kotelnik Theorem Impact on SOMA Algorithm Performance. In European Simulation Multiconference, 2005, Riga, ESM , 2005. p. 66-71. ISBN/ISSN: 1-84233-112-4.
- [7] ŠENKERÍK R., ZELINKA I., Optimization and Evolutionary Control of Chemical Reactor. In 10th International Research/Expert Conference Trends in the Development of Machinery and Associated Technology, TMT, Zenica, Bosnia and Hercegovina, 2006, p. 1171-1174. ISBN/ISSN: 9958-617-30-7.
- [8] Zelinka I., Umela inteligence v problemech globalni optimalizace. Praha, BEN – technicka literatura, 2002. ISBN 80-7300-069-5.
- [9] Zelinka I., Oplatkova, Z., Seda, M., Osmera, P., Vcelar, F., Evolucni vypocetni techniky – principy a aplikace. Praha, BEN – technicka literatura, 2008. ISBN 80-7300-218-3.
- [10] Varacha, P., Innovative Strategy of SOMA Control Parameter Setting. In 12th WSEAS International Conference on Neural Networks, Fuzzy Systems, Evolutionary Computing & Automation. Timisoara: WSEAS press, 2011, ISBN 978-960-474-292-9.876—880. Available: <http://www.halcyon.com/pub/journals/21ps03-vidmar>
- [11] VARACHA, P., JASEK, R., “ANN Synthesis for an Agglomeration Heating Power Consumption Approximation”. In Recent Researches in Automatic Control. Montreux : WSEAS Press, 2011, s. 239-244. ISBN 978-1-61804-004-6.
- [12] KOURIL, L., POSPISILIK, M., ADAMEK, M., JASEK, R., “Audio Transformers Optimization By Means of Evolutionary Algorithms”, In Proceedings of the 5th WSEAS World Congress on Applied Computing Conference, University of Algarve Faro, 2012, pp. 133 - 138, ISBN: 978-1-61804-089-3
- [13] KOURIL, L., POSPISILIK, M., ADAMEK, M., JASEK, R., “Coil Optimization with Aid of Flat Coil Optimizer”, In Proceedings of the 5th WSEAS World Congress on Applied Computing Conference, University of Algarve Faro, 2012, pp. 133 - 138, ISBN: 978-1-61804-089-3
- [14] X10. RESISTORS, online: <http://www.kpsec.freeuk.com/components/resist.htm>, cit. 14-05-2012.